Classical spins in topological insulators

Qin Liu[1] and Tianxing Ma[2]
[1]*Department of Physics, Fudan University, Shanghai 200433, China*
[2]*Max-Planck-Institut für Physik Komplexer Systeme, Nöthnitzer Strasse 38, 01187 Dresden, Germany*
(Received 13 January 2009; revised manuscript received 17 August 2009; published 29 September 2009)

Following the recent theoretical proposal and experiment on quantum spin Hall effect in HgTe/CdTe quantum wells, we consider a single magnetic impurity localized in the bulk of the system, which we treat as a classical spin. It is shown that there are always localized excited states in the bulk energy gap for arbitrarily strong impurity strength in the inverted region, while the localized excited states vanish for very strong impurity strength in the normal region. Similar conclusion also applies to three-dimensional topological insulators. This distinct difference serves as another criterion for the conventional and topological insulating phases when the time-reversal symmetry is broken, and can be easily experimentally observed through the scanning tunnel microscope and/or angle-resolved photoelectron spectroscopy experiments.

DOI: 10.1103/PhysRevB.80.115216 PACS number(s): 75.30.Hx, 73.20.At, 72.25.Dc

The quantum spin Hall (QSH) effect is a state of matter with topological properties distinct from those of conventional insulators.[1–3] The first proposal of experimental realization of this effect is given in the work by Bernevig *et al.*[3] where they consider the HgTe/CdTe semiconductor quantum wells (QWs), and show that when the thickness of the QW is varied, the electronic states change from a normal to an inverted type at a critical thickness d_c. This transition is a topological quantum phase transition between a conventional insulating phase and a phase exhibiting the QSH effect with a single pair of helical edge states. This phase transition can be understood by the relativistic Dirac model in (2+1) dimensions, which mimic the electronic states near the Γ point. At the quantum phase transition point, $d=d_c$, the mass term in the Dirac equation changes sign, leading to two distinct $U(1)$-spin and Z_2 topological numbers on either side of the transition. Recently, the QSH phase in HgTe/CdTe QWs has been observed in the transport experiments,[4] which confirms the theoretical predictions of Bernevig *et al.*[3]

Following this pioneer work, there emerge various discussions on the properties of the topological insulating phase in both two- and three-dimensional (2D, 3D) systems,[5–8] however, most of these are considered within the framework of the preservation of the time-reversal symmetry (TRS), among which, we notice that two of them show that the properties of this topological system can also be manifested by breaking the TRS on the surface through the so-called topological magnetoelectric effect[9] or local charge and spin density of states.[10] In the meanwhile, we notice that the system with Mn doped impurities in the bulk of the HgTe QWs has been discussed in Ref. 11, where by breaking the TRS in the bulk, the quantum anomalous Hall effect is realized. On the other hand, it is well-known that a single magnetic impurity in a superconductor breaks the TRS and induces low energy bound states in the superconducting gap.[12,13]

Motivated along this line, we discuss the presence of a single magnetic impurity located in the 2D bulk of the HgTe/CdTe QWs, which we treat as a classical spin in both normal and inverted regimes. Similar to the discussions in BCS superconductors by Shiba in 1968,[13] we show that in the inverted regime of the HgTe/CdTe QWs, there are always localized excited states (LES) in the bulk energy gap for arbitrarily strong impurity strength, while in normal regime, the LES vanish into the bulk for very strong impurity strength. This distinct difference of the response to the single magnetic impurity in bulk serves as another criteria for the conventional and topological insulating phases when the TRS is broken, and can be experimentally observed through the scanning tunnel microscope (STM) and/or angle-resolved photoelectron spectroscopy (ARPES) measurements.

The starting point of this paper is the effective four-band model[3] $H_0(\vec{k})=\varepsilon_k\sigma_0\tau_0+\mathcal{M}_k\sigma_0\tau_3+Ak_x\sigma_3\tau_1+Ak_y\sigma_0\tau_2$ in HgTe/CdTe QWs around the Γ point in the basis of $|E1,+\rangle$, $|H1,+\rangle$, $|E1,-\rangle$, and $|H1,-\rangle$, plus that of a short-range single magnetic impurity located at the origin. The exchange interaction in Mn doped HgTe QWs has been discussed in several literatures,[11,14] where it is established that the *s*-band and *p*-band electrons have different *sp-d* exchange coupling strength. To focus on the physical picture, we first consider the isotropic case where $J^s=J^p=J$, then the full Hamiltonian takes the form

$$H=\sum_k c_k^\dagger H_0(\vec{k})c_k+\frac{J}{2}\sum_{kk'} c_k^\dagger(\vec{S}\cdot\vec{\sigma})\tau_0 c_{k'}. \tag{1}$$

Here $\vec{S}$ is the spin vector of the magnetic impurity, and the Pauli matrix σ_i's act on spin space while τ_i's act on the two electric sub-bands space, σ_0 and τ_0 are both 2 by 2 unit matrices. We will show later that our result is robust for a general form of the exchange coupling. The full Green's function (GF) of Hamiltonian (1) is obtained through the equation of motion formulation[13] as

$$G_{kk'}(\omega)=G_k^0(\omega)\delta_{kk'}+G_k^0(\omega)t(\omega)G_{k'}^0(\omega), \tag{2}$$

where the t matrix takes the form

$$t(\omega)=\frac{\left(\frac{JS}{2}\right)^2 F(\omega)+\frac{J}{2}(\vec{S}\cdot\vec{\sigma})\tau_0}{1-\left[\frac{JS}{2}F(\omega)\right]^2}, \tag{3}$$

with $S^2=S_x^2+S_y^2+S_z^2$. In the above, we have introduced an F function as

$$F(\omega) = \frac{1}{N}\sum_k G_k^0(\omega) = \mathrm{diag}(F_e F_h F_e F_h), \tag{4}$$

where the diagonal elements are

$$F_{e(h)}(\omega) = \frac{1}{N}\sum_k \frac{\omega - \varepsilon_k + (-)\mathcal{M}_k}{D_k}. \tag{5}$$

In the tight-binding model, $\varepsilon_k = C - 2D(2 - \cos k_x - \cos k_y)$, $\mathcal{M}_k = M - 2B(2 - \cos k_x - \cos k_y)$, and $D_k = (\omega - \varepsilon_k - \mathcal{M}_k)(\omega - \varepsilon_k + \mathcal{M}_k) - A^2(\sin^2 k_x + \sin^2 k_y)$, where M, A, B, C, D are material parameters introduced in the effective four-band model in Ref. 3. Then the eigenenergies for the excited states are obtained by finding the poles of the GF in the bulk energy gap as

$$\frac{JS}{2} F_{e(h)}(\omega) = \pm 1, \tag{6}$$

which consists of four equations.

To characterize the momentum integration in both normal and inverted regimes, we notice that each diagonal block in $H_0(\vec{k})$ describes a quantum anomalous Hall system,[15] with the two forming a time-reversal conjugate pair. Using the result obtained by Qi *et al.*,[15] the topological behavior of this system is totally governed by two key parameters. In our case the correspondences are $e = -\frac{M}{2B} + 2$, which is related to the mass term in the (2+1)-D Dirac model, and $c = -\frac{2B}{A}$ which determines the sign of the Chern number. Therefore in the inverted regime we have $|e| < 2$ corresponding to $d > d_c$, otherwise it is topological trivial corresponding to a normal insulating phase. Furthermore, we set $\varepsilon_k = 0$ without loss of generality to obtain a particle-hole symmetric system, as we know that the quadratic kinetic term has no contribution to the topology of this system.[15]

We therefore rewrite Eq. (5) in terms of e and c, the result of which with ω in the bulk energy gap at several values of e parameter is shown in Fig. 1, where the topological nontrivial regime with $|e| < 2$ is given in the left column, while the trivial regime is plotted in the right column with $|e| > 2$. In each panel, the contribution from the electron sub-band, $F_e(\omega)$, is shown in red and that from the hole sub-band, $F_h(\omega)$, is shown in cyan. It is clear to see that the resonant condition, Eq. (6), is always satisfied for any given impurity strength J in the inverted regime, and there are four LES in the bulk gap, two come from the electron sub-band and two from the hole sub-band. Moreover, the stronger the impurity strength is, the nearer the LES are to the middle of the bulk gap, and no matter how strong the impurity strength is, there are always LES in the bulk gap which appear as peaks in the density of states (DOS).

In contrast, for the normal regime, we see that the resonant condition is *not* always satisfied for any impurity strength. For weak impurity strength, there could exist two LES near the gap edge, however, as we increase the impurity strength, these LES merge quickly into the bulk and vanish finally. That is, the peaks in the DOS in the bulk gap are not stable against the strong impurity strength for this case. This distinct difference of the response to the single magnetic impurity in bulk serves as another criteria for the conventional

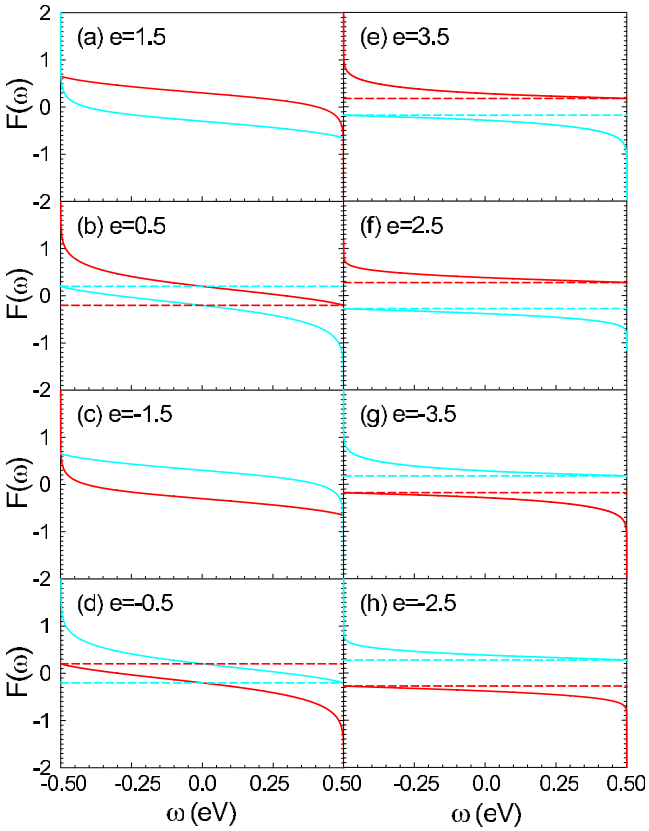

FIG. 1. (Color online) F function versus ω in the bulk-energy gap with several values of e and $c^2 = 1$. The topological nontrivial regime with $|e| < 2$ is shown in the left column, while the topological trivial regime with $|e| > 2$ is shown in the right column of the figure. $F_e(e, \omega)$ is plotted as red lines while $F_h(e, \omega)$ is plotted as cyan (gray) lines. The dotted lines are guidelines for the eyes to indicate the boundary values of the F functions.

and topological insulating phases when the TRS is broken. Note that this result is robust to the explicit form of the exchange interaction. For the Mn doped HgTe QWs,[11,14] we consider a form of exchange interaction, $J_z^{s(p)} S_z \sigma_z + J_\parallel^{s(p)}(S_x \sigma_x + S_y \sigma_y)$, in electron and hole bands separately. It turns out that the only difference with the isotropic model is to replace JS in Eq. (6) by $\sqrt{(J_z^{s,p})^2 S_z^2 + (J_\parallel^{s,p})^2 S_\parallel^2}$, and in the inverted region there are still four persistent LES in the gap, which never merge into the bulk.

To justify the above results obtained from t matrix method, we directly diagonalize the Hamiltonian (1) on a square lattice in both inverted and normal regimes by taking $e = 0.5$ and 3.5, for example. The obtained energy spectrum is plotted versus impurity strength in Fig. 2. The four persistent LES (red lines) in the bulk-energy gap are clearly shown for the nontrivial case where we see that they approach the middle of the gap as J increases and do not vanish. While in the trivial regime, there are only two LES for small J and merge into the bulk for large J. This result is in perfect agreement with the above analysis through GF discussions.

By using the real parameters of the HgTe/CdTe QWs system given in Ref. 3, we plot the F function at the quantum well width $d = 58$ Å and $d = 70$ Å, which are shown in Fig. 3. We see that for $d > d_c$ where the QSH effect is predicted,

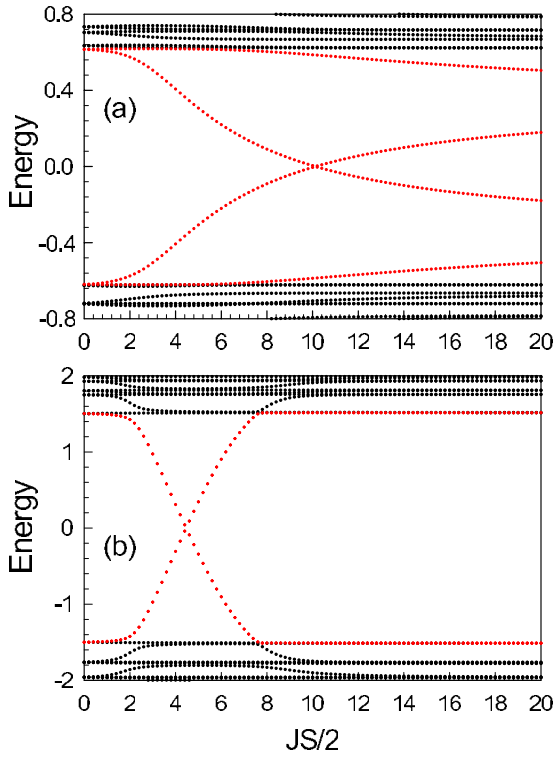

FIG. 2. (Color online) Energy spectrum obtained by direct diagonalization of Hamiltonian (1) with $\epsilon_k=0$ as a function of impurity strength in both (a) inverted and (b) normal regimes. The localized states are shown in red (intersecting lines in middle).

there are always LES in the bulk energy gap for arbitrarily strong impurity strength; while for $d<d_c$, which is a normal insulator, the LES vanish for strong impurity strength.

Considering that in real materials there is always a finite concentration of magnetic impurities, under which the localized excited states grow into impurity band, we estimate the critical concentration of magnetic impurities $\frac{1}{\tau_s M}$ in the topological nontrivial regime as a function of impurity strength $(1-\xi^2)^2/(1+\xi^2)^2$, at which the impurity band cannot be distinguished from the continuum, and the result is shown in Fig. 4. Here we have denoted $\xi=\frac{JS}{2}\pi N_F$ as the effective impurity strength and $\frac{1}{\tau_s M}=n_i\frac{JS}{M}\frac{\xi}{(1+\xi^2)^2}$ as the effective concentration. However we suggest that experimentally the actual concentration should be much lower than the critical values, so that not only its influence on the exchange coupling J is negligible,[14] but also the impurities can be considered isolated and their coupling, such as RKKY interactions, can be ignored. Furthermore, we speculate that our results should be still valid even within a complete quantum treatment of the magnetic impurity.[16]

Interestingly, the existence of LES in the bulk energy gap of a topological insulator is not special in two dimensions, but is also true for 3D strong topological insulators (STI). As an example, we consider the strained HgTe which is believed to be a STI.[9,17] The effect of magnetic impurities on the surface states of strained HgTe has been discussed by one of the authors,[10] here we focus on its effect in bulk. The model Hamiltonian describing strained HgTe with time-reversal as well as inversion symmetries takes the form[9,17]

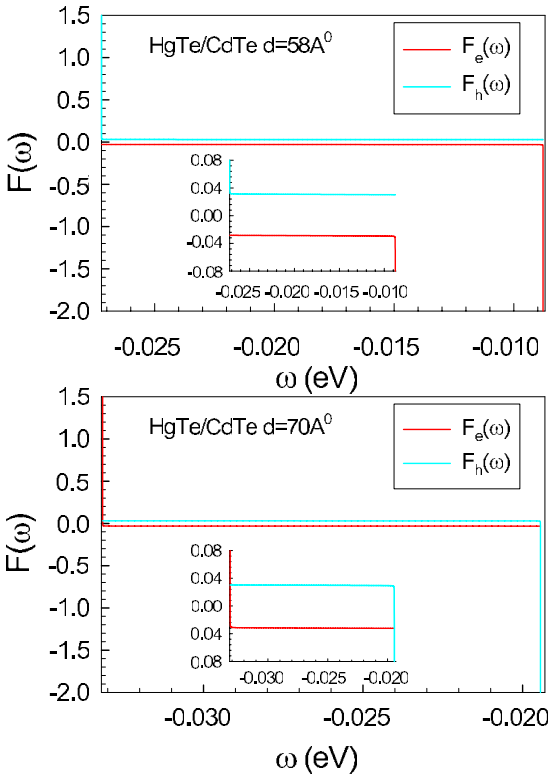

FIG. 3. (Color online) F function versus ω with ω in the bulk energy gap. The F functions are calculated numerically from Eq. (5) with the parameters taken from Ref. 3 for HgTe/CdTe QW at $d=58$ Å and $d=70$ Å. $F_e(\omega)$ are shown as red lines while $F_h(\omega)$ are shown as cyan lines. Inset: the enlarged structures for the nontrivial regime.

$$H_{3D}(\vec{k})=\mathcal{M}_k\Gamma^1+A_\perp k_x\Gamma^5+A_\perp k_y\Gamma^2+A_\parallel k_z\Gamma^3, \qquad (7)$$

where $\mathcal{M}_k=M_0-M_1(k_x^2+k_y^2)-M_2k_z^2$, and the representation for Gamma matrices is chosen in such a way that they are invariant under the joint transformations of inversion and time-reversal symmetries.[18] Two features are worth noticing

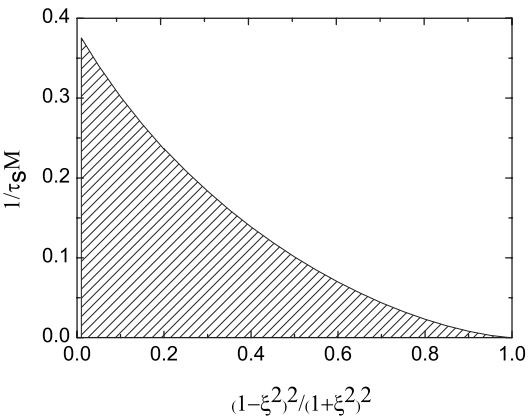

FIG. 4. Effective impurity concentration $\frac{1}{\tau_s M}$ as a function of effective impurity strength $(1-\xi^2)^2/(1+\xi^2)^2$. The shaded area indicates the range of the impurity concentration where the impurity band and the continuum are separated.

about this model Hamiltonian. First, by setting $A_{\parallel}=0$, Eq. (7) recovers the 2D HgTe/CdTe QW model. As we have discussed in the above, there are always LES in the inverted regime for arbitrarily strong impurity strength. Second, by comparing Eq. (7) with the Kane model[19] in the basis of $|E,\frac{1}{2}\rangle$, $|LH,-\frac{1}{2}\rangle$, $|E,-\frac{1}{2}\rangle$, $|LH,\frac{1}{2}\rangle$, we observe that they have exactly the same form. Therefore the matrix form for Kondo-like *sp-d* exchange term,[11,14,19] $H_{ex}(\vec{r})=-\Sigma_m J(\vec{r}-\vec{R}_m)\vec{S}_m\cdot\vec{\sigma}$, in the same basis can be similarly extracted as

$$H_{ex}=\begin{pmatrix} -\Delta_s e_z & 0 & -\Delta_s e_- & 0 \\ 0 & \frac{1}{3}\Delta_p e_z & 0 & -\frac{2}{3}\Delta_p e_+ \\ -\Delta_s e_+ & 0 & \Delta_s e_z & 0 \\ 0 & -\frac{2}{3}\Delta_p e_- & 0 & -\frac{1}{3}\Delta_p e_z \end{pmatrix}, \quad (8)$$

where $\Delta_s=yN_0J_s\langle S\rangle$, $\Delta_p=yN_0J_p\langle S\rangle$,[14] and $\vec{e}$ is the unit vector along the direction of impurity spin.

Following the methods developed by Fu and co-workers on 3D topological insulators with inversion symmetries,[7,20] the STI phase characterized by an odd number of Dirac points (k_x,k_y) in the 2D surface states of Hamiltonian (7) can be analyzed through two parameters $r=M_2/M_1$ and $r_1=M_0/4M_1$. Though we wouldn't elaborate the results in general, some specific examples are listed below. On a square lattice, for $r=1.5$, there is one Dirac point at (0,0) for $r_1=0.75$; three Dirac points at (0,0), $(0,\pi)$ and $(\pi,0)$ for $r_1=1.25$; the three Dirac points then move to $(0,\pi)$, $(\pi,0)$, and (π,π) for $r_1=2.25$; while for $r_1=3$ there is only one Dirac point again at (π,π). For even larger r_1 the system evolves out of the STI phase.

Using the same formulation,[13] the full GF for the system $H=\Sigma_k c_k^\dagger H_{3D}(\vec{k})c_k+\Sigma_{kk'}c_k^\dagger H_{ex}c_{k'}$ is obtained by finding the t matrix as

$$t_{3D}(\omega)=\frac{H_{ex}}{1-H_{ex}F(\omega)}, \quad (9)$$

where again the results in Eqs. (4) and (5) are recovered [$\epsilon_k=0$ automatically here since there are no kinetic terms in the Dirac Hamiltonian (7)] with $\mathcal{M}_k=M_0-2M_1(2-\cos k_x-\cos k_y)-2M_2(1-\cos k_z)$ and $D_k=\omega^2-[\mathcal{M}_k^2+2A_\perp^2(2-\cos k_x-\cos k_y)+2A_\parallel^2(1-\cos k_z)]$ in the 3D case. The resonant conditions for LES are obtained similarly by finding the poles of the full GF in the bulk energy gap as

$$\Delta_s F_e(\omega)=\pm 1, \quad \frac{\Delta_p\sqrt{4-3e_z^2}}{3}F_h(\omega)=\pm 1. \quad (10)$$

By numerically plotting $F_{e(h)}$ as a function of ω in the bulk energy gap, similar behavior as shown in Fig. 1 is found, respectively, for STI and non-STI phases using the values of r and r_1 illustrated above. We see that the same conclusion applies to 3D topological insulators. In the STI phase there are always LES in the bulk energy gap for arbitrary exchange interaction strength, while when out of STI phase, the LES exist only for very weak exchange interaction strength. Therefore we believe that the existence of nonvanishing LES in the bulk energy gap for arbitrary impurity strength plays the role of a general characterization for topological insulators.

Experimentally we suggest to detect this effect in the recently achieved HgTe/CdTe QWs[3,4] by doping a small concentration of Mn^{+2} ions in bulk. Since the LES evolve with the combination of exchange coupling strength and the magnetic moments (at the mean-field level), though it is hard to adjust the impurity exchange coupling strength, it may possible to tune the Mn moments by a small magnetic field.[11,14] When the Mn moments are larger than some critical value, there will be four peaks in the DOS spectrum in STM measurements for the QW width $d>d_c$, which persist for even larger polarization. When $d<d_c$, the peaks in the DOS spectrum will be broadened and vanish as the increasing in the polarization. However, for 3D STI systems with impurities doped deep in bulk, ARPES measurements will be more appropriate. We suggest to use this distinct signal to differentiate experimentally the topological and the conventional insulating phases.

The authors thank Shou-Cheng Zhang and Chao-Xing Liu for many illuminating discussions. Q.L. acknowledges the support of the China Scholarship Council for support. This work is supported by HKSAR RGC under Project No. CUHK 401806.

[1] C. L. Kane and E. J. Mele, Phys. Rev. Lett. **95**, 146802 (2005); **95**, 226801 (2005).
[2] B. A. Bernevig and S. C. Zhang, Phys. Rev. Lett. **96**, 106802 (2006).
[3] B. A. Bernevig, T. L. Hughes, and S.-C. Zhang, Science **314**, 1757 (2006).
[4] M. Konig, S. Wiedmann, C. Brune, A. Roth, H. Buhmann, L. W. Molenkamp, X.-L. Qi, and S.-C. Zhang, Science **318**, 766 (2007).
[5] J. E. Moore and L. Balents, Phys. Rev. B **75**, 121306(R) (2007).
[6] R. Roy, Phys. Rev. B **79**, 195321 (2009).
[7] L. Fu, C. L. Kane, and E. J. Mele, Phys. Rev. Lett. **98**, 106803 (2007).
[8] L. Fu and C. L. Kane, Phys. Rev. Lett. **100**, 096407 (2008).
[9] X.-L. Qi, T. L. Hughes, and S.-C. Zhang, Phys. Rev. B **78**, 195424 (2008).
[10] Q. Liu, C.-X. Liu, C. Xu, X.-L. Qi, and S.-C. Zhang, Phys. Rev. Lett. **102**, 156603 (2009).
[11] C.-X. Liu, X.-L. Qi, Xi Dai, Z. Fang, and S.-C. Zhang, Phys. Rev. Lett. **101**, 146802 (2008).
[12] L. Yu, Acta Phys. Sin. **21**, 75 (1965).
[13] H. Shiba, Prog. Theor. Phys. **40**, 435 (1968).
[14] E. G. Novik, A. Pfeuffer-Jeschke, T. Jungwirth, V. Latussek, C. R. Becker, G. Landwehr, H. Buhmann, and L. W. Molenkamp,

Phys. Rev. B **72**, 035321 (2005).

[15] X.-L. Qi, Y.-S. Wu, and S.-C. Zhang, Phys. Rev. B **74**, 085308 (2006).

[16] J. Zittartz and E. Müller-Hartmann, Z. Phys. **232**, 11 (1970); J. Zittartz, *ibid.* **237**, 419 (1970).

[17] X. Dai, T. L. Hughes, X.-L. Qi, Z. Fang, and S.-C. Zhang, Phys. Rev. B **77**, 125319 (2008).

[18] Explicitly, we take the time-reversal operator as $\mathcal{T}=\sigma^0\otimes i\tau^2 K$, where K is the complex conjugation, and the inversion operator $\hat{P}=\sigma^z\otimes\tau^0$. Under these definitions, the Gamma matrices which are invariant under the joint transformations of inversion and time-reversal symmetries are $\Gamma^1=\sigma^3\otimes\tau^0$, $\Gamma^2=\sigma^2\otimes\tau^0$, $\Gamma^{3,4,5}=\sigma^1\otimes\tau^{1,2,3}$.

[19] R. Winkler, *Spin-Orbit Coupling Effects in Two-Dimensional Electron and Hole Systems* (Springer-Verlag, Heidelberg, 2003).

[20] L. Fu and C. L. Kane, Phys. Rev. B **76**, 045302 (2007).